

Journal of Materials Chemistry C

Accepted Manuscript



This is an *Accepted Manuscript*, which has been through the Royal Society of Chemistry peer review process and has been accepted for publication.

Accepted Manuscripts are published online shortly after acceptance, before technical editing, formatting and proof reading. Using this free service, authors can make their results available to the community, in citable form, before we publish the edited article. We will replace this *Accepted Manuscript* with the edited and formatted *Advance Article* as soon as it is available.

You can find more information about *Accepted Manuscripts* in the [Information for Authors](#).

Please note that technical editing may introduce minor changes to the text and/or graphics, which may alter content. The journal's standard [Terms & Conditions](#) and the [Ethical guidelines](#) still apply. In no event shall the Royal Society of Chemistry be held responsible for any errors or omissions in this *Accepted Manuscript* or any consequences arising from the use of any information it contains.

Polymer composites of Boron Nitride Nanotubes and Nanosheets

Cite this: DOI: 10.1039/x0xx00000x

Wenjun Meng,^a Yang Huang,^a Yuqiao Fu,^a Zifeng Wang,^a and Chunyi Zhi^{*ab}Received 00th January 2012,
Accepted 00th January 2012

DOI: 10.1039/x0xx00000x

www.rsc.org/

Hexagonal boron nitride (h-BN) is a layered material with planer networks of BN hexagons, which is flexible to form various nanostructures. This feature article begins with an overall introduction of BN nanostructures and their novel properties, such as electrical insulating properties, high thermal conductivity, great mechanical strength, optical properties and so on. Then a comprehensive review of polymer composites of BN nanostructures with distinguished properties for different applications is presented. Finally, the problems of using BN nanostructures for the fabrication of polymer composites are discussed.

1. Introduction

As an analogue of carbon, boron nitride (BN) is a traditional material which is attracting more and more attentions in the nano-era. The layered structure of hexagonal BN makes it flexible to form various nanostructures, such as BN nanotubes (BNNTs),¹⁻⁶ BN nanosheets (BNNSs),⁷⁻¹¹ BN nanohorns^{12, 13} and BN spherical nanoparticles (BNNPs)^{14, 15} etc. After the first discovery of BNNTs by Zettl *et al.*,¹ many efforts have been made to improve the synthesis of BN nanostructures. Recent progress on mass production of these BN nanomaterials has paved a way to their applications, especially to the composite material studies.^{4, 16, 17}

The common novel properties of BN nanostructures, such as constant wide band gap,¹⁸ superb anti-oxidation ability and structural stability,^{19, 20} high thermal conductivity²¹⁻²³ and great mechanical properties,²⁴⁻²⁷ make BN nanostructures suitable as fillers for polymer composites to achieve higher thermal conductivity and mechanical strength. Although these applications seem quite similar to their corresponding carbon materials, BN nanostructures possess their uniqueness. For example, different from the black color of carbon-polymer composites, BN nanostructures-polymer composites can be white or even transparent,²⁸ which makes it feasible to dye the composites into different colors. Moreover, addition of carbon nanostructures ruins the electrical insulation of polymers, while BN nanostructure can keep their good dielectric properties or even improve their break over voltages.

Compared with traditional micro-size BN particle fillers, the nanostructured BN developed in recent years brings new attractive points due to their high aspect ratio, very high thermal conductivity and mechanical strength etc. The advantages of nano-sized BN compared with traditional BN are originated from their maximally exposed (002) atomic lattice plane with high performance, as shown in Figure 1. An example is that even though the (002) lattice plane of BN may possess high thermal conductivity up to thousands of W/mK, an average thermal conductivity of only tens of W/mK can be utilized when traditional BN micro-size particles are used as fillers. However, when the BNNTs, BNNSs and BNNPs are used,

the exposure of (002) lattice planes are maximized, which enables the utilization of the in-plane high thermal conductivity. In case of mechanical properties, the morphology of BN nanostructures avoids exfoliation of BN particles, which guarantees a fantastic tensile strength along axis of BNNTs or plane of BNNSs. Moreover, as fillers for polymer composites, the BN nanostructures also keep merits of traditional BN micro-sized particles, such as white color, superb anti-oxidation ability etc.

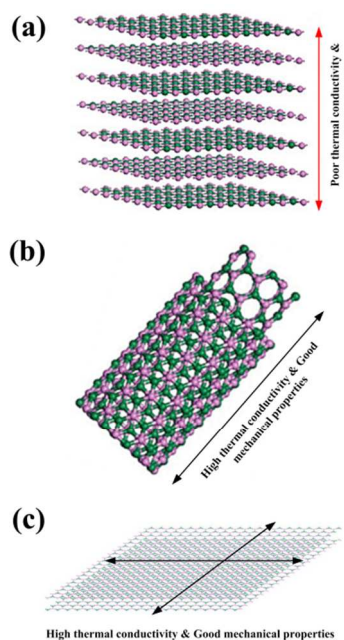


Fig. 1 High performance of nano-sized BN compared to traditional BN due to their maximally exposed (002) atomic lattice plane. (a) BN particles, (b) BNNTs and (c) BNNSs.

In this feature article, we will first introduce novel properties of BN nanostructure, as well as their advantage as fillers for polymer composites compared with traditional BN micro-size particles. Then a variety of polymer composites of BN nanostructures will be reviewed based on their different applications, followed by conclusions and perspectives.

2. Properties of BN nanostructures

Novel properties and their unique combinations are essentially fundamental to enable BN nanostructures as fillers for polymers and consequently achieve improvements of their performance. For example, the high thermal conductivity and electrical resistivity make BN nanostructures promising fillers for highly thermally conductive and electrically insulating polymer composites with excellent overall performance. The very high Young's modulus of BN nanostructures are often used for mechanical reinforcement of polymers. Therefore, here we briefly describe physical properties of BN nanostructures as follows from the point view of using them as fillers for polymer composites, a related summary is present in Table I.

2.1 Electrical properties of BN nanostructures

It is well known that BN materials possess a constant wide band gap of 5.8 eV (in some reports, it can be larger than 6.0 eV even),^{29,32} which induces an intrinsic electrically insulating property. Although some researchers observed conductive BNNTs, it is suggested this is caused by not-well-controlled doping during synthesis.^{33, 34} Direct experimental evidence for electrically insulation was demonstrated for BNNTs and BNNSs.^{33, 35, 36}

Bai *et al.* firstly experimentally demonstrated a piezoelectric behavior in BNNTs through investigating deformation driven electrical transport in such nanotubes.³⁷ However, it should not be a problem for fabricating electrically insulating polymer composites because even if the nanotubes are dramatically deformed, the current keeps at nA level with tens of volts applied. On the contrary, a very recent molecular dynamics simulation revealed that the polarization effects of BNNTs may induce a much stronger adhesion of polymers to BNNTs than to carbon nanotubes (CNTs).³⁸ The authors claimed that the composite materials of BNNTs and conjugated polymers have a potential application in the preparation of fibers with mechanical strength much higher than that of composite materials of CNTs and conjugated polymers due to much better interfacial strength than that in CNT-polymer composites.

Although few reports revealed that BNNSs can be electrically conductive due to defects and edge effects,^{33, 39, 40} BNNSs are considered as the best dielectric material in most cases for graphene based electronic devices. Therefore, it is believed that the intrinsic electrically insulating characteristic of BN can be well kept in BNNSs as long as there are no high concentration defects, doping or very strong edge effects due to very narrow ribbon morphology. Therefore, BN nanostructures are suitable for polymer composites with tunable dielectric properties.

2.2 Thermal properties of BN nanostructures

Superb anti-oxidation ability and structural stability are the prominent merits of BN nanostructures compared with other nanostructures, especially carbon nanostructures. As shown in Figure 2, the BNNTs can stand up to 800 °C in air, while the stability of CNTs in air is much worse.^{20, 41, 42} Moreover, AFM and Raman spectroscopy analyses reveal that monolayer BNNSs can sustain up to 850 °C, and the starting temperature of oxidation of BNNSs only slightly increases with the increase of nanosheet layer.⁴³ This

characteristic makes BN nanostructures much more suitable to work under oxidation environments and be used as high-performance oxidation-resistant coatings.⁴⁴ It was also reported that under vacuum conditions, the BN nanostructures can be structurally stable up to 3000 °C.⁴⁵ It should be noted that a strong electric field can remarkably decrease the breakdown temperature of individual BNNTs, that is, BNNTs can be decomposed at 1000-1700°C due to partially ionic nature of the B-N bonds.⁴⁶ However, it is suggested that this unfavorable point may not induce negative effects on any polymer composite application of BN nanostructures.

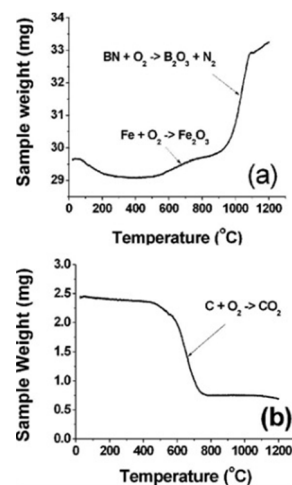


Fig. 2 Thermogravimetry (TGA) results of (a) BNNTs and (b) CNTs in air indicating much higher anti-oxidation ability of BNNTs (adapted from ref. 41).

The most unique property of electrically insulating BN nanostructures is their high thermal conductivity due to intensive phonon conductivity. It was theoretically predicted that BNNTs might possess a thermal conductivity up to 6000 W/mK,⁴⁷⁻⁴⁹ while actually no serious calculations were done to support this prediction. Zettl *et al.* carried out the first experimental study on thermal conductivity of BNNTs.²¹⁻²³ As shown in Figure 3, multi-walled BNNTs with a diameter of around 40 nm have a thermal conductivity of ~200W/mK at room temperature. Moreover, the diameter dependence of thermal conductivity of BNNTs is qualitatively similar to CNTs, with a higher thermal conductivity at a decreased diameter.^{22, 50} Isotopically pure ¹¹B BNNTs may have a 50% increase in thermal conductivity, which is very close to CNTs. However, it should be noted that the thermal conductivity of nanotubes depends on their diameter: smaller diameter, higher thermal conductivity. Therefore, it is believed that single-walled BNNTs with diameter of several nanometers may reach a thermal conductivity of thousands of W/mK, which is verified in Zettl's work by comparing diameter dependence of thermal conductivity of CNTs and BNNTs.²² A mat of BNNTs exhibits a very low thermal conductivity of 1.5 W/mK, which is suggested to be induced by extremely high interfacial thermal resistance. To avoid the negative effect, a model was established to roughly estimate thermal conductivity of individual BNNTs and a range of 120–960 W/mK was found^{51, 52}.

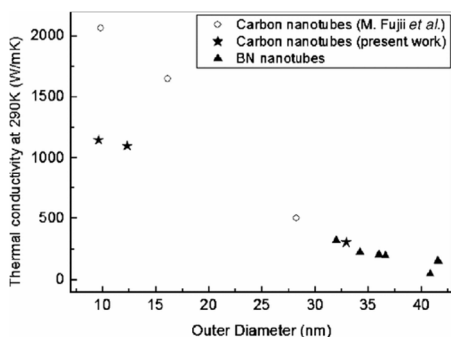


Fig. 3 Thermal conductivity vs outer diameter of various BNNTs (solid triangles) and CNTs (solid stars). Data shown by open circles are from ref. 48. It should be noted that the data for BNNTs and CNTs by this work maybe comparable because the experimental conditions are same (adapted from ref. 22).

Nanosheet structures have received extensive attentions after the discovery of graphene. Currently all investigations on thermal conductivity of BNNSs are theoretical works. Sevik *et al.* investigated the thermal transport properties of BN nanoribbons using equilibrium molecular dynamics.⁵³ It was revealed that BN nanostructures have considerably high thermal conductivities. Even though, it is still much lower than the carbon-based counterparts. For example, the room temperature lattice thermal conductivity of BNNSs are only around 400 W/mK, which is close to the value observed in metals, but much lower than graphene's 2500 W/mK. However, in some other theoretical studies using the nonequilibrium Green's functions method,^{54, 55} a thermal conductivity of 1700–3000 W/mK for BNNSs were demonstrated. The much lower thermal conductivity of BNNSs compared with that of carbon-based counterparts predicted by molecular dynamics might be caused by the strong phonon scattering restricts in classical molecular dynamics method. In the other theoretical studies, a reduction in such scattering in the single layer BNNSs arising mainly from a symmetry-based selection rule leads to a substantial increase in thermal conductivity compared with h-BN crystal, with calculated room temperature values of more than 600 W/mK. Isotopic enrichment can further increase thermal conductivity of BNNSs.^{56, 57}

Although the reported results for thermal conductivity of BN nanostructures are rather scattered, it is no doubt that BN nanostructures are very attractive for improving thermal conductivity of polymers. Combined with their intrinsic electrically insulating characteristics, BN nanostructures, especially single-walled BNNTs or single-layered BNNSs are considered to be the best fillers for highly thermally conductive and electrically insulating polymer composites.

2.3 Mechanical properties of BN nanostructures

BNNTs possess very high Young's modulus although it is slightly smaller than that of CNTs. A Young's modulus of 0.837 to 0.912 TPa was revealed in many theoretical works.^{24, 58–61} Moreover, it was predicted that at high temperatures or extremely long deformation times, BNNTs become more thermomechanically stable than CNTs due to higher formation energies in BNNTs than CNTs. There is a large scatter in the reported experimental data of elastic modulus of BNNTs. For example, Zetl *et al.* reported an axial Young's modulus of 1.22 TPa for BNNTs synthesized by arc-discharge method²⁴, which is even higher than theoretical data. For the BNNTs fabricated by chemical vapor deposition method using boron and metal oxide as reactants, the elastic modulus is around 722 GPa²⁷ (electric-field-induced resonance method) or 0.5–0.6 TPa²⁶ (TEM-atomic force

microscope method). The discrepancy is thought to be induced by different methods adopted.

A couple of theoretical models were proposed to investigate mechanical properties of BNNSs. However, the results were dependent very much on the models proposed.^{62–64} Li *et al.* presented a systematic experimental study on bending modulus of BNNSs produced by exfoliation method.⁶⁵ As shown in Figure 4, the bending moduli were found to increase with a decrease in sheet thickness and approach the theoretical C33 value (31.2 GPa) of a bulk hexagonal BN for sheet thicknesses below 50 nm. The strongly thickness-dependent bending modulus was attributed to the layer distribution of stacking faults. These studies indicate BN nanostructures are suitable for mechanical reinforcement of polymers. Thin BNNTs and BNNSs with low defects concentration and stacking faults are thought to be the best candidates for the fabrication of polymer composites to obtain mechanical reinforcement.

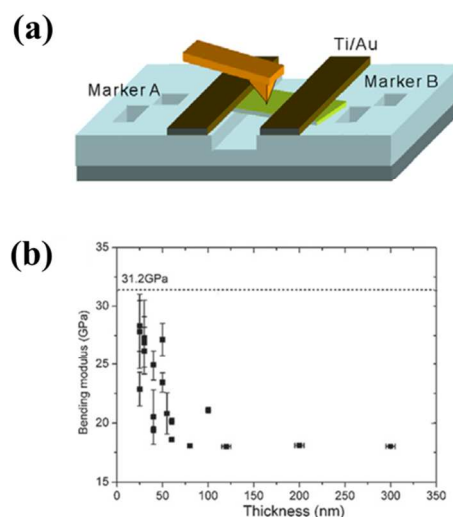


Fig. 4 (a) Schematic diagram of an AFM bending test of a clamped BNNS. (b) Bending modulus vs BNNSs thickness. The theoretical C33 literature value reported for a bulk h-BN (dashed line) is also shown for comparison (adapted from ref. 65).

2.4 Optical properties of BN nanostructures

Due to the well-investigated constant wide band gap, BN nanostructures usually possess a pure white appearance as long as there are not too many impurities, such as boron powder etc., included in the product. For the multi-walled BNNTs, a single absorption peak centered at 5.8 eV was observed,⁶⁶ while for single-walled BNNTs, two optical transitions at 4.45 and 5.5 eV were observed.³¹ BNNTs may emit effective violet and ultra-violet light under excitation of light (photoluminescence) or electron beams (cathodoluminescence). The detailed wavelengths of light emission depend largely on the fabrication and purification method of BNNTs. Usually, the broad emission peak at around 320 nm can be easily observed,^{30, 32, 67–72} which can be attributed to impurity and defect centers or to radiative excitonic dark states. The peak at around 225 nm induced by near band-gap excitonic recombination can also be observed sometimes in samples with high quality.^{32, 73, 74} Other emissions, such as emission at a wavelength of 460 nm, sometimes appear in the doped or surface oxidized samples.⁷⁵

The BNNSs possess very similar optical properties, including UV-vis absorption and luminescence properties with BNNTs.^{9, 76–79} Actually most BNNSs reported were fabricated by exfoliating h-BN

micro-sized particles and most BNNSs powder used for optical investigations are not thin enough to observe the quantum effects, the optical properties of BNNSs are also very close to micro-sized BN particles.

The optical properties of BNNTs and BNNSs make them a unique choice for fabrication of visible light transparent polymer film blocking ultra-violet light. Moreover, an embedment of BNNTs or BNNSs in the polymer matrix may give rise to ultra-violet light emission composite materials.

2.5 Other properties

Wetting is the ability of a liquid to maintain contact with a solid surface, resulting from intermolecular interactions at the interface. Although bulk BN surfaces can be relatively wetted by water, BN nanostructures have very poor wetting properties. Yum and Yu evaluated the static contact angle of water on BNNTs to be 85° by adopting the Wilhelmy method,⁸⁰ which is similar to that of water on graphite. In the case of other BN nanostructures, such as BNNSs, micromikes, submicrofunnels, etc., morphology and surface roughness play an important role in tuning the wetting properties.^{78, 81-83} The BNNS coatings with controllable levels of water repellency could be obtained from partial hydrophilicity with contact angles of 50° to superhydrophobicity with contact angles exceeding 150° .^{84, 85} BN nanostructure films are highly potential materials to find industrial applications in water-repelling, anti-corrosion and self-cleaning systems.

BNNSs that possess quite high specific surface area exhibit good performance in adsorbing oils, organic solvents and dyes from water while repelling water, which is of great importance in wastewater treatment process. Zhang *et al.* prepared ultrathin BNNSs via a variable-pressure one-step chemical synthesis route, displaying a maximum adsorption capacity of 436 mg/g for the organic dye methylene blue (MB) with the high surface area of $182 \text{ m}^2/\text{g}$.⁸⁶ Furthermore, Lei *et al.* increased the specific surface area of BN nanostructures to $1427 \text{ m}^2/\text{g}$ by introducing pores in BNNSs.⁸⁷ The synthesis process relied on a dynamic templating approach, during which the pores were created by gas bubbles released from the decomposition of the solid framework (hydrochloride guanidine). As shown in Figure 5, the resultant porous BNNSs show excellent adsorption performances with mass uptakes reaching 3300%, due to a combination of superhydrophobicity, porosity and swelling ability. Li *et al.* also prepared porous BN nanostructures with a ribbon-like structure and a super high surface area of $2078 \text{ m}^2/\text{g}$ and a large pore volume of $1.66 \text{ cm}^3/\text{g}$, by introducing structure-directed agent (P123) in a thermal decomposition of the BN precursor.⁸⁸ The obtained material was named as "activated BN", exhibiting a maximum adsorption capacity of 305 mg/g. Moreover, the saturated materials can be cleaned for reuse by simply washing, burning or heating in air thanks to their strong resistance to oxidation, rendering them promising materials for a wide range of applications in water purification and treatment.

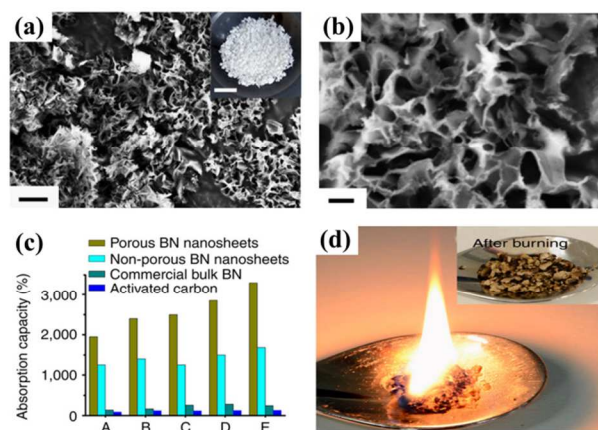


Fig. 5 (a) Low-magnification SEM image of the porous BNNSs (scale bar, 2 μm). Inset: photograph of the as-prepared porous BNNSs (scale bar, 1 cm). (b) High-magnification SEM image showing the porous structure of the as-prepared BNNSs (scale bar, 200 nm). (c) Comparison of the adsorption capacities of the porous BNNSs with non-porous BNNSs, commercial bulk BN particles and activated carbon. (d) Photograph of burning saturated porous BNNSs in air to remove the adsorbed oil, inset showing the color change after burning (adapted from ref. 87).

BNNTs could also be applied in hydrogen storage process by either physical or chemical adsorption mechanisms. The pioneering work of BNNTs for hydrogen uptake was reported by Ma *et al.*,⁸⁹ which demonstrated a 1.8-2.6 wt.% hydrogen uptake by multi-walled BNNTs under $\sim 10 \text{ MPa}$ at room temperature. Subsequently, Tang *et al.* synthesized BNNTs with collapsed structures, which possess a higher hydrogen adsorption capacity of 4.2 wt.%.⁹⁰ However, in the case of Tang's experiment, platinum nanoparticles found in the collapsed BNNTs product, which resulted from the synthetic procedure, may be a reason for the increase of the hydrogen uptake ability. Later on, it was indeed demonstrated that modifications of the BNNTs surface with some metals and/or intermetallic compounds have prominent hydrogen affinity, for instance, LaNi_5 may significantly improve electrochemical hydrogen storage of BNNTs.⁹¹

Studies on the biocompatibility of BN nanostructures are still at a very early stage.⁹²⁻⁹⁴ The pioneering work on biocompatibility of BN nanostructures were carried out by Ciofani *et al.* for *in vitro* tests of BNNTs on a human neuroblastoma cell line.^{95, 96} In their experiments, they wrapped BNNTs with polyethylenimine (PEI) to make them disperse well in the cell culture medium. The cells maintain a good viability after treatment with $5.0 \mu\text{g}/\text{mL}$ of PEI-BNNTs, indicating good biocompatibility of PEI-BNNTs which renders them suitable for biological applications. Moreover, the shortened BNNTs, which were obtained by breaking the sturdy structures of the BNNTs through a slow oxidation process, were found to possess good solubility in water and demonstrate remarkable improved DNA loading capacity.²⁰ Furthermore, Ciofani *et al.* performed the first preliminary *in vivo* toxicity evaluation of BNNTs following intravenous injection of glycol chitosan (GC)-coated BNNTs ($1 \text{ mg}/\text{kg}$ BNNTs) in five rabbits.⁹⁷ Although the number of animals tested in their study is small, the absence of negative effects on blood parameters as well as liver and kidney functions imply that BNNTs may be promising for biomedical and clinical applications.

3. Fabrication of BN nanostructures

A variety of synthesis methods have been utilized for the fabrication of BN nanostructures, most of which are similar to the

well-established techniques for the preparation of the corresponding carbon nanostructures, with slight modifications. In this section, some of the most important methods developed for the growth of BN nanostructures, especially BNNTs and BNNSs, are briefly reviewed.

The first successful fabrication of BNNTs was reported by Zettl *et al.* via an arc-discharge between a BN-packed tungsten rod and a cooled copper electrode.¹ In the following attempts for the growth of BNNTs, various fabrication methods, such as modified arc-discharge,^{5, 98-100} autoclave,¹⁰¹⁻¹⁰³ template synthesis,¹⁰⁴⁻¹⁰⁶ plasma-jet method,^{107, 108} laser ablation,^{6, 17, 109-111} ball-milling¹¹²⁻¹¹⁵ and chemical vapor deposition,¹¹⁶⁻¹¹⁹ were utilized. Herein, we will specially describe a so-called BOCVD method developed by Bando and his colleagues,^{16, 117} due to its feasibility of a routine gram-quantity BNNTs production. In a typical BOCVD process, a mixture of B and MgO was loaded into a BN crucible at the bottom of the reaction chamber in a vertical induction furnace. The mixture was used as reactant and heated to approximately 1300 °C to form a highly reactive B₂O₃ and Mg vapors, which were subsequently argon-transported into a reaction chamber and reacted with supplying ammonia in the lower temperature furnace zone. This method separates a boron precursor (boron powder plus metal oxide) from the as-grown BNNTs during the growth, which could protect BNNTs from contamination by the precursors and guarantee their ultimate purity. Various metal oxides were found to be effective for the BNNTs' growth in the BOCVD process. A mixture of MgO and FeO or MgO and SnO was found to be the best.¹⁶

BNNSs were first prepared by decomposition of borazine in the form of so-called nanomeshes on metallic substrates in the case of lattice mismatch.¹²⁰ Since the similar lattice structure of BNNSs and graphene, the well-known mechanical and/or chemical exfoliation techniques utilized for the growth of graphene were also used for the preparation of mono- and few-layered BNNSs. Two major methods were utilized for the mechanical exfoliation process. One is to peel off layers of BN with an adhesive tape;¹²¹⁻¹²³ the other is to exfoliate BN by ultrasonication.^{124, 125} In a typical chemical exfoliation process, molten hydroxides have been used to obtain few-layered BNNSs.¹²⁶ The exfoliation process involves the following sequence: (1) self-curling of the sheets at the edges due to the adsorption of cations (Na⁺ or K⁺) on the outmost BN surface; (2) anions and cations entering the interlayer space and the adsorption of anions (OH⁻) on the positively curved surface which drives continuous curling of the BN layer; (3) direct peeling away from the parent materials, or cutting by the reaction of BN surface with hydroxides. Moreover, other techniques such as chemical blowing¹²⁷ and substitution reactions¹²⁸ were also reported to be effective in the production of BNNSs.

4. Polymer composites of BN nanostructures

4.1 Polymer functionalized BN nanostructures

BNNTs are hardly dispersed in water and most organic solvents. First exploration on fabrication of soluble BNNTs were realized by wrapping BNNTs with amineterminated oligomeric poly(ethyleneglycol) (PEG1500N)¹²⁹ or poly[*m*-phenylenevinylene-co-(2,5-dioctoxyphenylenevinylene)] (PmPV).⁶⁶ The weak interaction utilized is electrostatic interaction between B sites on BNNTs and amino groups on backbone of PEG1500N or π stacking interaction between surfaces of BNNTs with PmPV. Soon afterwards, different polymers were found to be effective for functionalization of BNNTs for different purposes, including proteins,¹³⁰⁻¹³³ deoxyribonucleic acid (DNA),^{14, 134} peptide,¹³⁵ gum arabic,¹³² polyvinylpyrrolidone (PVP),^{20, 136, 137} polyethyleneimine,

^{95, 96} polyaniline,^{138, 139} poly(*p*-phenyleneethynylene)s (PPEs) and polythiophene¹⁴⁰ etc. The purposes of functionalizing BNNTs include better dispersibility in solvents, better interfacial interaction in composites materials,^{28, 42} better molecule loading ability,¹³² biological application explorations^{92, 141} and so on. It should be specially mentioned that a molecular dynamics (MD) simulation approach was used to investigate the interfacial binding of BNNTs with PmPV, polystyrene (PS), and polythiophene (PT).³⁸ Interestingly enough, the comparison of results for BNNT-polymer composites with those of the similar carbon nanotube (CNT)-polymer composites reveals that the BNNT-polymer interactions are much stronger. This finding is also in good agreement with recent experimental observations.¹³⁸⁻¹⁴⁰ The stronger interfacial binding of polymers to BNNTs is suggested to be caused by the surface polarization of BNNTs, which directly gives rise to the strong electrostatic interactions between them, while only van der Waals interactions govern the interface of CNT-polymers.

Studies on polymer functionalized BNNSs are very few so far, since there is no need to modify the BNNSs by polymers before their applications. The BNNSs fabricated by a sonication method usually have functional groups attached, which results in the decent dispersibility of BNNSs in the solvent. In a pioneering work of BNNSs synthesis done by Han *et al.*,⁸ PmPV was used as surfactant to make the liquid exfoliation more effective. It is believed that the π stacking interaction between aromatic structures in PmPV and *h*-BN surface plays an important role during the exfoliation.

4.2 Mechanical reinforcement by BN nanostructures

Excellent mechanical properties of *h*-BN along (002) lattice plane make BNNTs and BNNSs suitable for mechanical reinforcement of polymers. The present author firstly used BNNTs synthesized by a chemical vapor deposition method at high temperature to improve mechanical properties of polystyrene.²⁸ It was found with 1 wt% pristine BNNTs, the elastic modulus of polystyrene can be 7% improved, while with assistant of PmPV as surfactant, a more effective improvement was achieved. This work demonstrated BNNTs can be an enhancer for polymers, while many critical issues were revealed. For example, without adding PmPV, the mechanical properties of polystyrene, either elastic modulus or strength became even worse when chloroform was used as solvents, which indicates a very poor dispersibility and interfacial interaction between polymer and pristine BNNTs. The best datum achieved in this work is 21% improvement of elastic modulus with 1 wt% BNNTs. Moreover, it was revealed that at low fraction of BNNTs embedment, the transparency of polymer films can be well kept. Instead of functionalization through weak π stacking interaction between PmPV and BNNTs, utilizing covalent modified BNNTs is obviously a better choice. We developed an effective facile method to fabricate a chemically activated BNNTs, which are hydroxylated and suitable for further modification through chemical reactions based on hydroxyl groups.¹⁴² The hydroxylated BNNTs were found to be much more effective for polymers' mechanical reinforcement compared to pristine BNNTs (Figure 6). For both polycarbonate (PC) and polyvinyl butyral (PVB), with a 1 wt% fraction of pristine BNNTs, the elastic modulus can be improved up to around 20% (e.g., PC, 13.6%; PVB, 25.0%). However, with hydroxylated BNNTs, the elastic modulus of PC is improved up to 31.8%, and for PVB, it is 36.5%. The yield strength of the polymers was also improved effectively. Hydroxylated BNNTs again show better results. The results when hydroxylated BNNTs were used were close to theoretical results, which verified that the hydroxylated BNNTs can effectively interact with a polymer. In the other works, modified BNNTs were also found to be much more effective for mechanical reinforcement of polymers.^{131, 143} For example, Young's modulus of

polyvinyl alcohol (PVA) increased up to 42% with 1 wt% isophoronediiisocyanate-modified BNNTs, while in case of pristine BNNTs used, the PVA became even weaker.

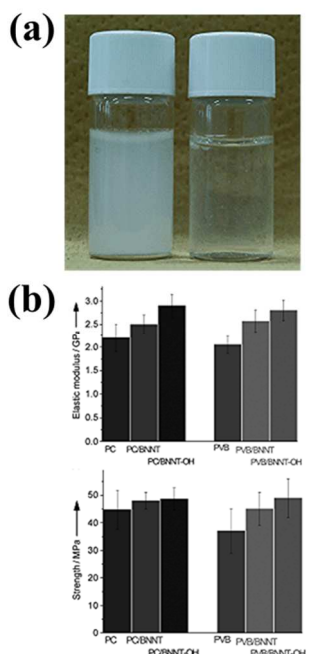


Fig. 6 (a) Photograph of an aqueous dispersion of hydroxylated BNNTs (left) and pristine BNNTs in water (right). (b) Comparative tensile tests performed on PC-BNNT and PVB-BNNT composites. Elastic modulus (upper). Yield strength (below). In each histogram, the bars from left to right represent a pure polymer, a pristine BNNT-polymer composite, and a hydroxylated BNNT-polymer composite, respectively (adapted from ref. 142).

The mechanical properties of BNNSs were investigated by nanoindentation measurements¹⁴⁴ and three-point bending tests⁶⁵ using AFM, showing an elastic modulus in the range of 200-500 N/m and a thickness dependence of bending modulus. The pioneering work of exfoliating BN powder for the large-scale fabrication of 2D BNNSs was carried out in our previous group by a sonication-centrifugation technique¹²⁴. The as-prepared BNNS was applied to fabricate PMMA/BNNSs transparent composites, in which a 22% improvement in the elastic modulus of PMMA and an 11% increase in its strength were obtained with only 0.3 wt% BNNSs fraction utilized (Figure 7). Later on, Coleman's group also exfoliated BN by ultrasonication in various solvents to give dispersions of BNNSs.¹²⁵ They prepared composites of liquid exfoliated BNNSs in a PVA matrix with a considerable mechanical reinforcement of 40% increase in modulus and strength relative to the pure polymer at volume fraction of only 0.12 vol%.¹⁴⁵ Moreover, the mechanical properties of BNNS-polymer composites could be further enhanced by uniaxial drawing, which might be attributed to strain-induced exfoliation or de-aggregation as well as alignment of BNNSs.¹⁴⁶ In addition, BNNSs prepared via chemical blowing¹²⁷ or substitution reaction of graphite powders¹²⁸ are also reported to be utilized to prepare BNNSs-polymer composites for the application of mechanical reinforcement of polymers.

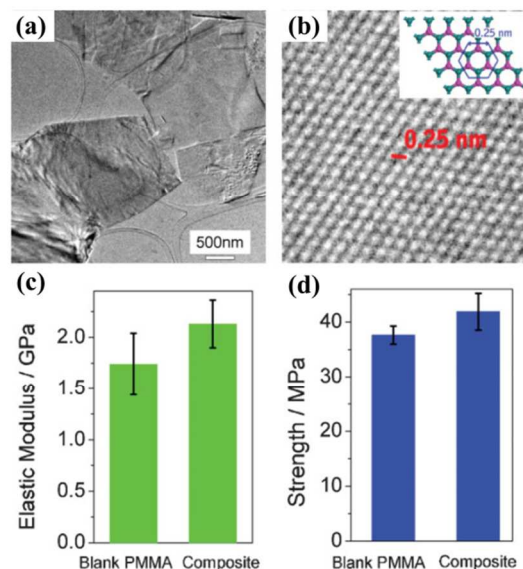


Fig. 7 (a) Low-magnification SEM image of BNNSs. (b) High-magnification TEM image of BNNSs with the incident electron beam is perpendicular to the (002) plane, inset showing structure model of BNNSs with a fringe separation of ~ 0.25 nm. (c) Elastic modulus and (d) strength of blank PMMA and its BNNSs composites (adapted from ref. 124).

4.3 Thermally conductive electrically insulating polymer composites

The most amazing characteristic of BN materials is that they are electrically insulating while thermally conductive, especially inside the (002) lattice plane. Electrons of BN are localized due to ionic properties of B-N bonds, while heat can be easily transferred through phonons. Actually, although no comprehensive practical applications due to relatively higher prices compared with other ceramic particles, such as alumina, SiC etc, the h-BN powder (usually micro-sized) has been widely investigated for fabrication of thermally conductive insulating polymer composites and proved to be one of the best filler for this application. Only in recent years, nano-sized BN, such as BNNTs and BNNSs were applied in the studies of highly thermally conductive insulating polymer composites and demonstrated to be very attractive.

Compared to micro-sized BN powder, BNNTs and BNNSs have their unique advantages to be used as fillers for highly thermally conductive insulating polymer composites. Inside (002) lattice plane, BN has a high thermal conductivity up to thousands of W/mK, while in the other lattice plane, it is low to several W/mK. Therefore, micro-sized BN powder provide an average effects on thermal transfer, while BNNTs and BNNSs can maximize the effects of (002) lattice plane by crimping or minimizing thickness of other lattice planes. Thus, it is believed that BNNTs and BNNSs are more effective for thermal conductivity improvement of polymer composites. Moreover, it is predicted that nano-sized fillers can form thermal conductive pathways more easily by connections between each other and thus are more effective in enhancing the thermal transfer in the polymer matrix.

Terao *et al.* fabricated BNNTs/polyvinyl formal (PVF) composite films containing high BNNT fraction of up to 10 wt% and improved the thermal conductivity of the polymer by $\sim 250\%$.¹⁴⁷ Utilizing an absorption process, BNNTs/polymer composites with high BNNT fractions were fabricated, showing a thermal conductivity of up to 3.61 W/mK and CTE value down to $16 \times 10^{-6} \text{ K}^{-1}$ from BNNTs-loaded PS and poly(ethylene vinyl alcohol) (PEVA) composites, respectively.¹⁴⁸ The present author applied sonication-exfoliated

BNNs to fabricate PMMA/BNNs transparent composites, in which a striking reduction of the coefficients of thermal expansion (CTE) was obtained, compared to the blank PMMA.¹²⁴ Later on, Song *et al.* exfoliated hexagonal BN to give sheets of nanoscale thickness and dispersed the resultant BNNs in PVA and epoxy matrices to get cast thin film with a considerably higher in-plane thermal conductivity, 30 W/mK with the volume loading of 50% BNNs.¹⁴⁹ Recently, a dielectric nanocomposite paper with 2D layered BNNs wired by 1D nanofibrillated cellulose (NFC) was reported to have a superior thermal conductivity of up to 145.7 W/mK for 50 wt % of BN along the BN paper surface due to the formation of BN percolating network.¹⁵⁰ As shown in Figure 8, 2D BNNs form a thermally conductive network along the surface of the composites, while 1D NFC used as a stabilizer provides mechanical strength. Moreover, hybrid fillers formed by combining 2D BNNs and 1D BNNTs could also improve the thermal conductivity of epoxy composites, due to the synergetic effect resulted from the generation of 3D thermal networks between BNNTs and BNNs.¹⁵¹

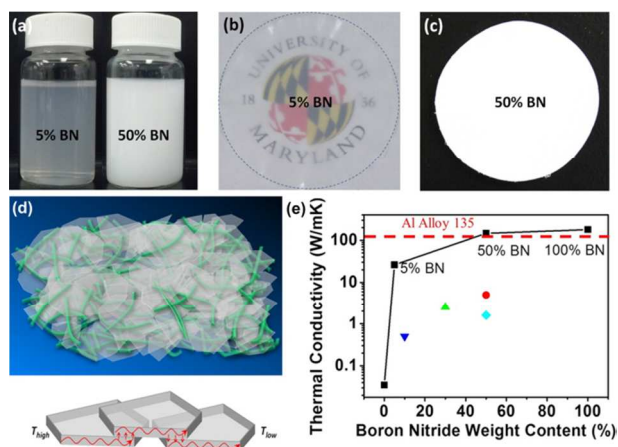


Fig. 8 (a) Images of the stable mixture with 5 wt% (left) and 50 wt% (right) BN. (b) An image of transparent and thermal conductive film with 5 wt% BN. (c) An image of white film with 50 wt% BN. (d) Schematic to show the structure of cellulose nanofiber with layered BN to transfer heat flux in the horizontal plane direction between BN layers. (e) Thermal conductivity of BN/NFC composites vs BN content (adapted from ref. 150).

At a given filler loading, the thermal conductivity of composites are not fully determined by the size and shape of the particles. Evidence has shown that surface modification of the particles, which tunes the interface interactions between the filler and the polymer matrix, is essential for high thermally conductive polymer composites.^{147, 152-155} For instance, Xu and Chung showed that the thermal conductivity of BN particle epoxy-matrix composites was increased by surface treatment of BN particles using acetone, HNO₃, H₂SO₄ and silane, in which silane treatment gave the best thermal conductivity of up to 10.3 W/mK at 57 vol% BN loading.¹⁵² Other than silane, PS and PMMA were coated on the BN surface via admicellar polymerization to increase the thermal conductivity of BN-filled epoxy composites.¹⁵³ In addition, other BN nanostructures, such as BN nanoplatelets non-covalent functionalization by octadecylamine (ODA) and covalent functionalization by hyperbranched aromatic polyamide (HBP)¹⁵⁴, and BNNTs modified with catechin¹⁴⁷ and polyhedral oligosilsesquioxane (POSS),¹⁵⁵ are applied as fillers for the fabrication of high thermally conductive polymer composites. After these treatments, the dispersibility of the fillers as well as the interface between filler and polymer matrix are

improved, resulting in an improvement in the thermal conductivity of the polymer composites.

Filler orientation and alignment in composites, which is of particular importance for the development of thermally anisotropic materials to improve the directional thermal properties of the composites, can be induced by selecting various processing method. By using an electric field, BNNs were aligned perpendicular to the surface of the epoxy¹⁵⁶ and polysiloxane¹⁵⁷ nanocomposite films plane. The resulting composite films with oriented BNNs manifested improved thermal diffusivity compared to the composites prepared without orientation. In addition, magnetic BN hybrid nanostructures decorated with iron oxide (γ -Fe₂O₃ or Fe₃O₄) could be used for manipulating the anisotropic properties of direction-dependent materials under a magnetic field.¹⁵⁸⁻¹⁶⁰ As shown in Figure 9, Fe₃O₄-coated magnetic h-BN particles randomly dispersed in an epoxy matrix are reoriented in a direction perpendicular to the substrate under a magnetic field. Due to the diamagnetic susceptibility along the c-axis, BNNs could also be aligned with high anisotropy either parallel or perpendicular to the polysiloxane composite film plane without surface modification by applying a high magnetic field.¹⁶¹ Furthermore, BNNTs in polymer composite fibers could be spontaneously aligned in the fiber casting direction during the fabrication process of the fibers by an electro-spinning method.¹⁶²

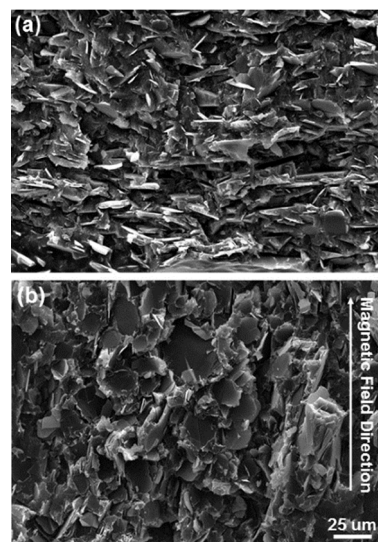


Fig. 9 Cross-sectional SEM images of Fe₃O₄-coated h-BN/epoxy composites aligned (a) randomly and (b) vertically to the film plane (adapted from ref. 160).

4.4 Other applications of BN nanostructure polymer composites

BN nanostructures are generally recognized as wide band gap (5.5-6.0 eV) semiconductors. Our previous research on dielectric and thermal properties of BNNTs/epoxy composites was the first report to use BNNTs to adjust dielectric properties of a polymer.¹⁶³ A significantly decreased dielectric constant and a 69% improvement of thermal conductivity were observed in the as-prepared BNNTs/epoxy composites. Recently, Huang *et al.* used POSS-modified BNNTs as nanofillers to fabricate dielectric epoxy composites with high thermal conductivity.¹⁵⁵ Thanks to the intrinsic low dielectric constant of embedded BNNTs and well-designed surface modifications, the obtained BNNTs epoxy composites exhibited a remarkably decreased dielectric constant and dielectric loss tangent (Figure 10). The achievements of the simultaneous properties of low dielectric constant, low dielectric loss, and high

thermal conductivity in BNNTs polymer composites may pave a way for comprehensive applications in electronic packaging and thermal management for energy systems.

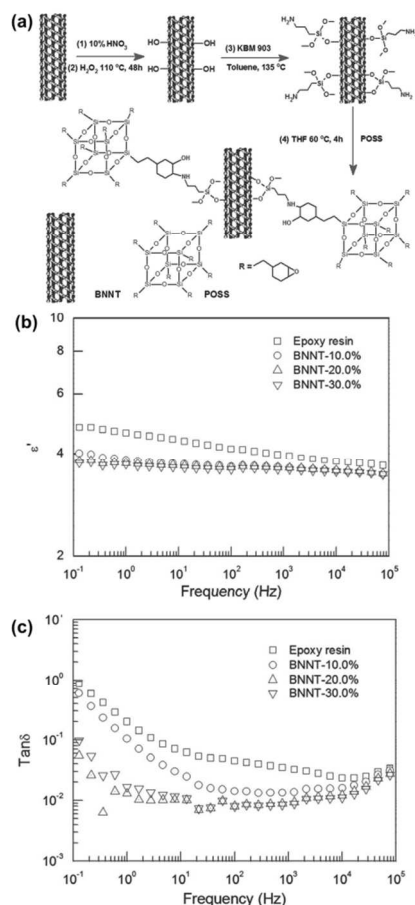


Fig. 10 (a) Schematic diagram illustrating a process of POSS modification on the surface of as-grown BNNTs. (b) Frequency-dependent dielectric constant of the epoxy/BNNTs-POSS composites. (c) Dielectric loss tangent of the epoxy/BNNTs-POSS composites (adapted from ref. 155).

Ravichandran *et al.* reported a Saran (a co-polymer of vinylidene chloride and acrylonitrile) based polymer BNNTs composites suitable for photovoltaic packaging application.¹⁶⁴ The obtained composites exhibited high transparency in the visible region, good barrier properties and thermal stability. In addition, chitosan/BN composites were prepared by solution technique using CuSO₄/glycine chelate complex as the catalyst.¹⁶⁵ A substantial reduction in oxygen permeability was observed with the increase of boron nitride concentrations, which might be promising in the packaging industry.

5. Conclusions and perspectives

The investigations on polymer composites of BN nanostructures are still at their very early stage. The limitation is mostly caused by the difficulties of large scale synthesis of BN nanostructures. Currently grams level BN nanotubes are available, while it is still difficult to carry out serious polymer composite studies. Most polymer composite samples of BNNTs are designed to be films or small size mat to control the dosage of the BNNTs. For BN nanosheets, although it seems liquid exfoliation is an effective method to produce large amount of samples, while the contradiction between yield and thickness was not solved perfectly so far. Most

BNNTs utilized for polymer composite fabrication possess graphene-like morphology but are much thicker than graphene.

As far as the fabrication process is concerned, the interface and dispersion, which are two major problems for composite materials, extensively exist in polymer composites of BN nanostructures. One reason is that, with one-dimensional or two-dimensional structures, the uniform dispersion of BN nanostructures gets more difficult than particles. The other reason is that, in comparison with carbon nanostructures which can utilize many well-established chemical reactions to realize effective surface modifications, the chemical reactions for B and N elements are much more limited. A universal method developed for modification to BN nanostructures is to oxidize B sites to get hydroxyl groups connected, followed by chemical reactions based on the hydroxyl groups. The other method is to hydrogenate the N sites and utilize the chemical reactions based on amino groups to modify the BN nanostructures.

The above mentioned problems make the performance achieved in the polymer composites of BN nanostructures are far behind of what are expected. Mechanical reinforcement can only be achieved at low fraction of BN nanostructures. At slightly high fraction, for example, higher than 5wt.%, the mechanical properties of polymers will be even ruined induced by poor dispersibility and poor interfacial interactions. On the other hand, effective thermal conductivity enhancement can only be achieved at high filler fraction. Recently BNNTs/polymer composites with a very high in-plane thermal conductivity were fabricated. This is a remarkable progress. However, the thermal conductivity of the composites is very anisotropic, which means that the thermal conductivity along the direction perpendicular to the composites sheets is very low. Therefore, how to form highly thermal conductive 3D paths in the composite material is a very important topic deserving more efforts. Polymer composite materials utilizing other properties of BN nanostructures, such as optical properties, irradiation properties and biocompatibilities are still very rare in literatures. It is not because the related research is not important or interesting, most likely, it is because the fabrication of BN nanostructures are still not easy, which hinders the progresses on their composite studies.

Acknowledgements

This research was supported by the Early Career Scheme of the Research Grants Council of Hong Kong SAR, China, under Project Numbers CityU9041977, the Science Technology and Innovation Committee of Shenzhen Municipality (Grant Number JCYJ20130401145617276), and a grant from the City University of Hong Kong.

Notes and references

- ^a Department of Physics and Materials Science, City University of Hong Kong, 83 Tat Chee Avenue, Kowloon, Hong Kong.
^b Shenzhen Research Institute, City University of Hong Kong, Shenzhen, P.R.China. E-mail: cy.zhi@cityu.edu.hk

- 1 N. G. Chopra, R. J. Luyken, K. Cherrey, V. H. Crespi, M. L. Cohen, S. G. Louie and A. Zettl, *Science*, 1995, **269**, 966-967.
- 2 C. Y. Zhi, Y. Bando, C. C. Tang and D. Golberg, *Mat Sci Eng R*, 2010, **70**, 92-111.
- 3 J. S. Wang, V. K. Kayastha, Y. K. Yap, Z. Y. Fan, J. G. Lu, Z. W. Pan, I. N. Ivanov, A. A. Puzetzy and D. B. Geohegan, *Nano Lett*, 2005, **5**, 2528-2532.

- 4 Y. Chen, J. F. Gerald, J. S. Williams and P. Willis, *Mater Sci Forum*, 1999, **312-314**, 173-178.
- 5 A. Loiseau, F. Willaime, N. Demoncey, N. Schramchenko, G. Hug, C. Colliex and H. Pascard, *Carbon*, 1998, **36**, 743-752.
- 6 D. Golberg, Y. Bando, M. Eremets, K. Takemura, K. Kurashima and H. Yusa, *Appl Phys Lett*, 1996, **69**, 2045-2047.
- 7 D. Golberg, Y. Bando, Y. Huang, T. Terao, M. Mitome, C. C. Tang and C. Y. Zhi, *ACS Nano*, 2010, **4**, 2979-2993.
- 8 W. Q. Han, L. J. Wu, Y. M. Zhu, K. Watanabe and T. Taniguchi, *Appl Phys Lett*, 2008, **93**, 223103.
- 9 Y. Lin, T. V. Williams and J. W. Connell, *J Phys Chem Lett*, 2010, **1**, 277-283.
- 10 Y. Lin, T. V. Williams, W. Cao, H. E. Elsayed-Ali and J. W. Connell, *J Phys Chem C*, 2010, **114**, 17434-17439.
- 11 J. Yu, L. Qin, Y. F. Hao, S. Kuang, X. D. Bai, Y. M. Chong, W. J. Zhang and E. Wang, *ACS Nano*, 2010, **4**, 414-422.
- 12 C. Y. Zhi, Y. Bando, C. C. Tang and D. Golberg, *Phys Rev B*, 2005, **72**, 245419.
- 13 C. Y. Zhi, Y. Bando, C. C. Tang, D. Golberg, R. G. Xie and T. Sekiguchi, *Appl Phys Lett*, 2005, **87**, 63107-63109.
- 14 C. Y. Zhi, W. J. Meng, T. Yamazaki, Y. Bando, D. Golberg, C. C. Tang and N. Hanagata, *J Mater Chem*, 2011, **21**, 5219-5222.
- 15 C. C. Tang, Y. Bando, Y. Huang, C. Y. Zhi and D. Golberg, *Adv Funct Mater*, 2008, **18**, 3653-3661.
- 16 C. Y. Zhi, Y. Bando, C. C. Tang and D. Golberg, *Solid State Commun*, 2005, **135**, 67-70.
- 17 M. W. Smith, K. C. Jordan, C. Park, J. W. Kim, P. T. Lillehei, R. Crooks and J. S. Harrison, *Nanotechnology*, 2009, **20**, 505604.
- 18 X. Blase, A. Rubio, S. G. Louie and M. L. Cohen, *EPL-Europhys Lett*, 1994, **28**, 335-340.
- 19 Y. Chen, J. Zou, S. J. Campbell and G. Le Caer, *Appl Phys Lett*, 2004, **84**, 2430-2432.
- 20 C. Y. Zhi, N. Hanagata, Y. Bando and D. Golberg, *Chem-Asian J*, 2011, **6**, 2530-2535.
- 21 A. Zettl, C. W. Chang and G. Begtrup, *Phys Status Solidi B*, 2007, **244**, 4181-4183.
- 22 C. W. Chang, A. M. Fennimore, A. Afanasiev, D. Okawa, T. Ikuno, H. Garcia, D. Y. Li, A. Majumdar and A. Zettl, *Phys Rev Lett*, 2006, **97**, 085901.
- 23 C. W. Chang, W. Q. Han and A. Zettl, *Appl Phys Lett*, 2005, **86**, 173102.
- 24 N. G. Chopra and A. Zettl, *Solid State Commun*, 1998, **105**, 297-300.
- 25 E. Hernandez, C. Goze, P. Bernier and A. Rubio, *Phys Rev Lett*, 1998, **80**, 4502-4505.
- 26 D. Golberg, P. Costa, O. Lourie, M. Mitome, X. D. Bai, K. Kurashima, C. Y. Zhi, C. C. Tang and Y. Bando, *Nano Lett*, 2007, **7**, 2146-2151.
- 27 A. P. Suryavanshi, M. F. Yu, J. G. Wen, C. C. Tang and Y. Bando, *Appl Phys Lett*, 2004, **84**, 2527-2529.
- 28 C. Y. Zhi, Y. Bando, C. C. Tang, S. Honda, H. Kuwahara and D. Golberg, *J Mater Res*, 2006, **21**, 2794-2800.
- 29 J. C. Charlier, X. Blase and S. Roche, *Rev Mod Phys*, 2007, **79**, 677-732.
- 30 C. Y. Zhi, Y. Bando, C. C. Tang, D. Golberg, R. G. Xie and T. Sekigushi, *Appl Phys Lett*, 2005, **86**, 213110.
- 31 J. S. Lauret, R. Arenal, F. Ducastelle, A. Loiseau, M. Cau, B. Attal-Tretout, E. Rosencher and L. Goux-Capes, *Phys Rev Lett*, 2005, **94**, 037405.
- 32 P. Jaffrennou, J. Barjon, T. Schmid, L. Museum, A. Kanaev, J. S. Lauret, C. Y. Zhi, C. Tang, Y. Bando, D. Golberg, B. Attal-Tretout, F. Ducastelle and A. Loiseau, *Phys Rev B*, 2008, **77**, 235422.
- 33 H. B. Zeng, C. Y. Zhi, Z. H. Zhang, X. L. Wei, X. B. Wang, W. L. Guo, Y. Bando and D. Golberg, *Nano Lett*, 2010, **10**, 5049-5055.
- 34 M. Radosavljevic, J. Appenzeller, V. Derycke, R. Martel, P. Avouris, A. Loiseau, J. L. Cochon and D. Pigache, *Appl Phys Lett*, 2003, **82**, 4131-4133.
- 35 Y. Huang, S.-L. Yue, C.-Z. Gu, C. C. Tang, Y. Bando, F. F. Xu and D. Golberg, *Wuli*, 2005, **34**, 791-792.
- 36 C. Y. Zhi, Y. Bando, C. C. Tang and D. Golberg, *Phys Rev B*, 2006, **74**, 153413.
- 37 X. D. Bai, D. Golberg, Y. Bando, C. Y. Zhi, C. C. Tang, M. Mitome and K. Kurashima, *Nano Lett*, 2007, **7**, 632-637.
- 38 A. T. Nasrabadi and M. Foroutan, *J Phys Chem B*, 2010, **114**, 15429-15436.
- 39 V. Barone and J. E. Peralta, *Nano Lett*, 2008, **8**, 2210-2214.
- 40 W. Chen, Y. F. Li, G. T. Yu, C. Z. Li, S. B. B. Zhang, Z. Zhou and Z. F. Chen, *J Am Chem Soc*, 2010, **132**, 1699-1705.
- 41 C. Ying, Z. Jin, S. J. Campbell and G. Le Caer, *Appl Phys Lett*, 2004, **84**, 2430-2432.
- 42 C. Y. Zhi, Y. Bando, C. C. Tang, Q. Huang and D. Golberg, *J Mater Chem*, 2008, **18**, 3900-3908.
- 43 L. H. Li, J. Cervenka, K. Watanabe, T. Taniguchi and Y. Chen, *ACS Nano*, 2014, **8**, 1457-1462.
- 44 Z. Liu, Y. J. Gong, W. Zhou, L. L. Ma, J. J. Yu, J. C. Idrobo, J. Jung, A. H. MacDonald, R. Vajtai, J. Lou and P. M. Ajayan, *Nat Commun*, 2013, **4**.
- 45 F. P. Bundy and R. H. Wentorf, *J Chem Phys*, 1963, **38**, 1144.
- 46 Z. Xu, D. Golberg and Y. Bando, *Nano Lett*, 2009, **9**, 2251-2254.
- 47 S. Berber, Y. K. Kwon and D. Tomanek, *Phys Rev Lett*, 2000, **84**, 4613-4616.
- 48 C. W. Chang, D. Okawa, H. Garcia, A. Majumdar and A. Zettl, *Phys Rev Lett*, 2008, **101**, 075903.
- 49 Y. Xiao, X. H. Yan, J. Xiang, Y. L. Mao, Y. Zhang, J. X. Cao and J. W. Ding, *Appl Phys Lett*, 2004, **84**, 4626-4628.
- 50 M. Fujii, X. Zhang, H. Q. Xie, H. Ago, K. Takahashi, T. Ikuta, H. Abe and T. Shimizu, *Phys Rev Lett*, 2005, **95**, 065502.
- 51 C. W. Chang, W. Q. Han and A. Zettl, *J Vac Sci Technol B*, 2009, **27**, 199-199.
- 52 C. C. Tang, Y. Bando, C. H. Liu, S. S. Fan, J. Zhang, X. X. Ding and D. Golberg, *J Phys Chem B*, 2006, **110**, 10354-10357.
- 53 C. Sevik, A. Kinaci, J. B. Haskins and T. Cagin, *Phys Rev B*, 2011, **84**, 085409.
- 54 K. K. Yang, Y. P. Chen, Y. E. Xie, X. L. Wei, T. Ouyang and J. X. Zhong, *Solid State Commun*, 2011, **151**, 460-464.
- 55 O. Y. Tao, Y. P. Chen, Y. E. Xie, K. K. Yang, Z. G. Bao and J. X. Zhong, *Nanotechnology*, 2010, **21**, 245701.
- 56 L. Lindsay and D. A. Broido, *Phys Rev B*, 2011, **84**, 155421.
- 57 L. Lindsay and D. A. Broido, *Phys Rev B*, 2012, **85**, 035436.
- 58 E. Hernandez, C. Goze, P. Bernier and A. Rubio, *Appl Phys Mater*, 1999, **68**, 287-292.

- 59 Y. J. Peng, L. Y. Zhang, Q. H. Jin, B. H. Li and D. T. Ding, *Physica E*, 2006, **33**, 155-159.
- 60 V. Verma, V. K. Jindal and K. Dharamvir, *Nanotechnology*, 2007, **18**.
- 61 H. F. Bettinger, T. Dumitrica, G. E. Scuseria and B. I. Yakobson, *Phys Rev B*, 2002, **65**, 041406.
- 62 L. Boldrin, F. Scarpa, R. Chowdhury and S. Adhikari, *Nanotechnology*, 2011, **22**, 505702.
- 63 J. H. Yuan and K. M. Liew, *J Nanosci Nanotechno*, 2012, **12**, 2617-2624.
- 64 Q. Peng, W. Ji and S. De, *Comp Mater Sci*, 2012, **56**, 11-17.
- 65 C. Li, Y. Bando, C. Y. Zhi, Y. Huang and D. Golberg, *Nanotechnology*, 2009, **20**, 385707.
- 66 C. Y. Zhi, Y. Bando, C. C. Tang, R. G. Xie, T. Sekiguchi and D. Golberg, *J Am Chem Soc*, 2005, **127**, 15996-15997.
- 67 P. Jaffrenou, F. Donatini, J. Barjon, J. S. Lauret, A. Maguer, B. Attal-Tretout, F. Ducastelle and A. Loiseau, *Chem Phys Lett*, 2007, **442**, 372-375.
- 68 P. Jaffrenou, J. Barjon, J. S. Lauret, A. Maguer, D. Golberg, B. Attal-Tretout, F. Ducastelle and A. Loiseau, *Phys Status Solidi B*, 2007, **244**, 4147-4151.
- 69 Z. G. Chen, J. Zou, Q. F. Liu, C. H. Sun, G. Liu, X. D. Yao, F. Li, B. Wu, X. L. Yuan, T. Sekiguchi, H. M. Cheng and G. Q. Lu, *ACS Nano*, 2008, **2**, 1523-1532.
- 70 Z. G. Chen, J. Zou, G. Liu, F. Li, H. M. Cheng, T. Sekiguchi, M. Gu, X. D. Yao, L. Z. Wang and G. Q. Lu, *Appl Phys Lett*, 2009, **94**, 023105.
- 71 H. Chen, Y. Chen, C. P. Li, H. Z. Zhang, J. S. Williams, Y. Liu, Z. W. Liu and S. P. Ringer, *Adv Mater*, 2007, **19**, 1845-1848.
- 72 B. Berzina, L. Trinkler, R. Krutovostov, R. T. Williams, D. L. Carroll, R. Czerw and E. Shishonok, *Physica Status Solidi C*, 2005, 318-321.
- 73 L. Wirtz, A. Marini and A. Rubio, *Phys Rev Lett*, 2006, **96**, 126104.
- 74 C. H. Park, C. D. Spataru and S. G. Louie, *Phys Rev Lett*, 2006, **96**, 126105.
- 75 C. C. Tang, Y. Bando, C. Y. Zhi and D. Golberg, *Chem Commun*, 2007, 4599-4601.
- 76 R. Gao, L. W. Yin, C. X. Wang, Y. X. Qi, N. Lun, L. Y. Zhang, Y. X. Liu, L. Kang and X. F. Wang, *J Phys Chem C*, 2009, **113**, 15160-15165.
- 77 L. H. Li, Y. Chen, B. M. Cheng, M. Y. Lin, S. L. Chou and Y. C. Peng, *Appl Phys Lett*, 2012, **100**, 261108.
- 78 A. Pakdel, X. B. Wang, C. Y. Zhi, Y. Bando, K. Watanabe, T. Sekiguchi, T. Nakayama and D. Golberg, *J Mater Chem*, 2012, **22**, 4818-4824.
- 79 Z. Y. Zhao, Z. G. Yang, Y. Wen and Y. H. Wang, *J Am Ceram Soc*, 2011, **94**, 4496-4501.
- 80 K. Yum and M. F. Yu, *Nano Lett*, 2006, **6**, 329-333.
- 81 M. C. Gordillo and J. Marti, *Phys Rev E*, 2011, **84**, 011602.
- 82 A. Pakdel, Y. Bando and D. Golberg, *Langmuir*, 2013, **29**, 7529-7533.
- 83 H. Li and X. C. Zeng, *ACS Nano*, 2012, **6**, 2401-2409.
- 84 A. Pakdel, C. Y. Zhi, Y. Bando, T. Nakayama and D. Golberg, *ACS Nano*, 2011, **5**, 6507-6515.
- 85 A. Pakdel, X. B. Wang, Y. Bando and D. Golberg, *Acta Mater*, 2013, **61**, 1266-1273.
- 86 S. J. Zhang, G. Lian, H. B. Si, J. Wang, X. Zhang, Q. L. Wang and D. L. Cui, *Journal of Materials Chemistry A*, 2013, **1**, 5105-5112.
- 87 W. W. Lei, D. Portehault, D. Liu, S. Qin and Y. Chen, *Nat Commun*, 2013, **4**, 1777.
- 88 J. Li, X. Xiao, X. W. Xu, J. Lin, Y. Huang, Y. M. Xue, P. Jin, J. Zou and C. C. Tang, *Sci Rep*, 2013, **3**, 3208.
- 89 R. Z. Ma, Y. Bando, H. W. Zhu, T. Sato, C. L. Xu and D. H. Wu, *J Am Chem Soc*, 2002, **124**, 7672-7673.
- 90 C. C. Tang, Y. Bando, X. X. Ding, S. R. Qi and D. Golberg, *J Am Chem Soc*, 2002, **124**, 14550-14551.
- 91 X. Chen, X. P. Gao, H. Zhang, Z. Zhou, W. K. Hu, G. L. Pang, H. Y. Zhu, T. Y. Yan and D. Y. Song, *J Phys Chem B*, 2005, **109**, 11525-11529.
- 92 G. Ciofani, V. Raffa, J. Yu, Y. Chen, Y. Obata, S. Takeoka, A. Menciasci and A. Cuschieri, *Curr Nanosci*, 2009, **5**, 33-38.
- 93 G. Ciofani, *Expert Opinion on Drug Delivery*, 2010, **7**, 889-893.
- 94 G. Ciofani, S. Danti, G. G. Genchi, B. Mazzolai and V. Mattoli, *Small*, 2013, **9**, 1672-1685.
- 95 G. Ciofani, V. Raffa, A. Menciasci and A. Cuschieri, *Biotechnol Bioeng*, 2008, **101**, 850-858.
- 96 G. Ciofani, V. Raffa, A. Menciasci and P. Dario, *J Nanosci Nanotechno*, 2008, **8**, 6223-6231.
- 97 G. Ciofani, S. Danti, G. G. Genchi, D. D'Alessandro, J. L. Pellequer, M. Odorico, V. Mattoli and M. Giorgi, *Int J Nanomed*, 2012, **7**, 19-24.
- 98 A. Loiseau, F. Willaime, N. Demoncey, G. Hug and H. Pascard, *Phys Rev Lett*, 1996, **76**, 4737-4740.
- 99 K. Suenaga, C. Colliex, N. Demoncey, A. Loiseau, H. Pascard and F. Willaime, *Science*, 1997, **278**, 653-655.
- 100 J. Cumings and A. Zettl, *Chem Phys Lett*, 2000, **316**, 211-216.
- 101 L. Q. Xu, Y. Y. Peng, Z. Y. Meng, W. C. Yu, S. Y. Zhang, X. M. Liu and Y. T. Qian, *Chem Mater*, 2003, **15**, 2675-2680.
- 102 G. Rosas, J. Sistos, J. A. Ascencio, A. Medina and R. Perez, *Appl Phys a-Mater*, 2005, **80**, 377-380.
- 103 J. Dai, L. Q. Xu, Z. Fang, D. P. Sheng, Q. F. Guo, Z. Y. Ren, K. Wang and Y. T. Qian, *Chem Phys Lett*, 2007, **440**, 253-258.
- 104 W. Q. Han, Y. Bando, K. Kurashima and T. Sato, *Appl Phys Lett*, 1998, **73**, 3085-3087.
- 105 D. Golberg, Y. Bando, K. Kurashima and T. Sato, *Chem Phys Lett*, 2000, **323**, 185-191.
- 106 M. Bechelany, S. Bernard, A. Brioude, D. Cornu, P. Stadelmann, C. Charcosset, K. Fiaty and P. Miele, *J Phys Chem C*, 2007, **111**, 13378-13384.
- 107 Y. Shimizu, Y. Moriyoshi, H. Tanaka and S. Komatsu, *Appl Phys Lett*, 1999, **75**, 929-931.
- 108 E. Bengu and L. D. Marks, *Phys Rev Lett*, 2001, **86**, 2385-2387.
- 109 T. Laude, Y. Matsui, A. Marraud and B. Jouffrey, *Appl Phys Lett*, 2000, **76**, 3239-3241.
- 110 D. P. Yu, X. S. Sun, C. S. Lee, I. Bello, S. T. Lee, H. D. Gu, K. M. Leung, G. W. Zhou, Z. F. Dong and Z. Zhang, *Appl Phys Lett*, 1998, **72**, 1966-1968.
- 111 R. Arenal, O. Stephan, J. L. Cochon and A. Loiseau, *J Am Chem Soc*, 2007, **129**, 16183-16189.
- 112 Y. Chen, L. T. Chadderton, J. FitzGerald and J. S. Williams, *Appl Phys Lett*, 1999, **74**, 2960-2962.

- 113 Y. Chen, M. Conway, J. S. Williams and J. Zou, *J Mater Res*, 2002, **17**, 1896-1899.
- 114 J. Yu, Y. Chen, R. Wuhler, Z. W. Liu and S. P. Ringer, *Chem Mater*, 2005, **17**, 5172-5176.
- 115 J. Kim, S. Lee, Y. R. Uhm, J. Jun, C. K. Rhee and G. M. Kim, *Acta Mater*, 2011, **59**, 2807-2813.
- 116 O. R. Lourie, C. R. Jones, B. M. Bartlett, P. C. Gibbons, R. S. Ruoff and W. E. Buhro, *Chem Mater*, 2000, **12**, 1808-1810.
- 117 C. Tang, Y. Bando, T. Sato and K. Kurashima, *Chem Commun*, 2002, 1290-1291.
- 118 C. C. Tang, Y. Bando, G. Z. Shen, C. Y. Zhi and D. Golberg, *Nanotechnology*, 2006, **17**, 5882-5888.
- 119 T. Terao, Y. Bando, M. Mitome, K. Kurashima, C. Y. Zhi, C. C. Tang and D. Golberg, *Physica E*, 2008, **40**, 2551-2555.
- 120 M. Corso, W. Auwarter, M. Muntwiler, A. Tamai, T. Greber and J. Osterwalder, *Science*, 2004, **303**, 217-220.
- 121 D. Pacile, J. C. Meyer, C. O. Girit and A. Zettl, *Appl Phys Lett*, 2008, **92**.
- 122 J. C. Meyer, A. Chuvilin, G. Algara-Siller, J. Biskupek and U. Kaiser, *Nano Lett*, 2009, **9**, 2683-2689.
- 123 R. V. Gorbachev, I. Riaz, R. R. Nair, R. Jalil, L. Britnell, B. D. Belle, E. W. Hill, K. S. Novoselov, K. Watanabe, T. Taniguchi, A. K. Geim and P. Blake, *Small*, 2011, **7**, 465-468.
- 124 C. Y. Zhi, Y. Bando, C. C. Tang, H. Kuwahara and D. Golberg, *Adv Mater*, 2009, **21**, 2889-2893.
- 125 J. N. Coleman, M. Lotya, A. O'Neill, S. D. Bergin, P. J. King, U. Khan, K. Young, A. Gaucher, S. De, R. J. Smith, I. V. Shvets, S. K. Arora, G. Stanton, H.-Y. Kim, K. Lee, G. T. Kim, G. S. Duesberg, T. Hallam, J. J. Boland, J. J. Wang, J. F. Donegan, J. C. Grunlan, G. Moriarty, A. Shmeliov, R. J. Nicholls, J. M. Perkins, E. M. Grievson, K. Theuvsissen, D. W. McComb, P. D. Nellist and V. Nicolosi, *Science*, 2011, **331**, 568-571.
- 126 X. Li, X. Hao, M. Zhao, Y. Wu, J. Yang, Y. Tian and G. Qian, *Adv Mater*, 2013, **25**, 2200-2204.
- 127 X. B. Wang, A. Pakdel, C. Y. Zhi, K. Watanabe, T. Sekiguchi, D. Golberg and Y. Bando, *J Phys-Condens Mat*, 2012, **24**, 314205.
- 128 F. Liu, X. S. Mo, H. B. Gan, T. Y. Guo, X. B. Wang, B. Chen, J. Chen, S. Z. Deng, N. S. Xu, T. Sekiguchi, D. Golberg and Y. Bando, *Sci Rep*, 2014, **4**, 4211.
- 129 S. Y. Xie, W. Wang, K. A. S. Fernando, X. Wang, Y. Lin and Y. P. Sun, *Chem Commun*, 2005, 3670-3672.
- 130 C. Zhi, Y. Bando, C. Tang and D. Golberg, *J Am Chem Soc*, 2005, **127**, 17144-17145.
- 131 V. K. Thakur, J. Yan, M. F. Lin, C. Y. Zhi, D. Golberg, Y. Bando, R. Sim and P. S. Lee, *Polym Chem-Uk*, 2012, **3**, 962-969.
- 132 Z. H. Gao, C. Y. Zhi, Y. Bando, D. Golberg, M. Komiyama and T. Serizawa, *Rsc Adv*, 2012, **2**, 6200-6208.
- 133 X. Chen, P. Wu, M. Rousseas, D. Okawa, Z. Gartner, A. Zettl and C. R. Bertozzi, *J Am Chem Soc*, 2009, **131**, 890-891.
- 134 C. Zhi, Y. Bando, W. Wang, C. Tang, H. Kuwahara and D. Golberg, *Chem-Asian J*, 2007, **2**, 1581-1585.
- 135 Z. H. Gao, C. Y. Zhi, Y. Bando, D. Golberg and T. Serizawa, *J Am Chem Soc*, 2010, **132**, 4976-4977.
- 136 Q. Huang, Y. S. Bando, X. Xu, T. Nishimura, C. Y. Zhi, C. C. Tang, F. F. Xu, L. Gao and D. Golberg, *Nanotechnology*, 2007, **18**, 485706.
- 137 Q. Huang, Y. Bando, A. Sandanayaka, C. C. Tang, J. B. Wang, T. Sekiguchi, C. Y. Zhi, D. Golberg, Y. Araki, O. Ito, F. F. Xu and L. Gao, *Small*, 2007, **3**, 1330-1335.
- 138 C. Y. Zhi, L. J. Zhang, Y. Bando, T. Terao, C. C. Tang, H. Kuwahara and D. Golberg, *J Phys Chem C*, 2008, **112**, 17592-17595.
- 139 C. Y. Zhi, Y. Bando, C. C. Tang, S. Honda, K. Sato, H. Kuwahara and D. Golberg, *Angew Chem Int Edit*, 2005, **44**, 7929-7932.
- 140 S. Velayudham, C. H. Lee, M. Xie, D. Blair, N. Bauman, Y. K. Yap, S. A. Green and H. Y. Liu, *Acs Appl Mater Inter*, 2010, **2**, 104-110.
- 141 G. Ciofani, V. Raffa, A. Menciassi and A. Cuschieri, *Nano Today*, 2007, 8-10.
- 142 C. Y. Zhi, Y. Bando, T. Terao, C. C. Tang, H. Kuwahara and D. Golberg, *Chem-Asian J*, 2009, **4**, 1536-1540.
- 143 S. J. Zhou, C. Y. Ma, Y. Y. Meng, H. F. Su, Z. Zhu, S. L. Deng and S. Y. Xie, *Nanotechnology*, 2012, **23**, 055708.
- 144 L. Song, L. J. Ci, H. Lu, P. B. Sorokin, C. H. Jin, J. Ni, A. G. Kvashnin, D. G. Kvashnin, J. Lou, B. I. Yakobson and P. M. Ajayan, *Nano Lett*, 2010, **10**, 3209-3215.
- 145 U. Khan, P. May, A. O'Neill, A. P. Bell, E. Boussac, A. Martin, J. Semple and J. N. Coleman, *Nanoscale*, 2013, **5**, 581-587.
- 146 R. Jan, P. May, A. P. Bell, A. Habib, U. Khan and J. N. Coleman, *Nanoscale*, 2014, **6**, 4889-4895.
- 147 T. Terao, Y. Bando, M. Mitome, C. Y. Zhi, C. C. Tang and D. Golberg, *J Phys Chem C*, 2009, **113**, 13605-13609.
- 148 C. Y. Zhi, Y. Bando, T. Terao, C. C. Tang, H. Kuwahara and D. Golberg, *Adv Funct Mater*, 2009, **19**, 1857-1862.
- 149 W. L. Song, P. Wang, L. Cao, A. Anderson, M. J. Meziani, A. J. Farr and Y. P. Sun, *Angew Chem Int Edit*, 2012, **51**, 6498-6501.
- 150 H. L. Zhu, Y. Y. Li, Z. Q. Fang, J. J. Xu, F. Y. Cao, J. Y. Wan, C. Preston, B. Yang and L. B. Hu, *ACS Nano*, 2014, **8**, 3606-3613.
- 151 J. L. Su, Y. Xiao and M. Ren, *Phys Status Solidi A*, 2013, **210**, 2699-2705.
- 152 Y. S. Xu and D. D. L. Chung, *Compos Interface*, 2000, **7**, 243-256.
- 153 K. Wattanakul, H. Manuapiya and N. Yanumet, *J Appl Polym Sci*, 2011, **119**, 3234-3243.
- 154 J. H. Yu, X. Y. Huang, C. Wu, X. F. Wu, G. L. Wang and P. K. Jiang, *Polymer*, 2012, **53**, 471-480.
- 155 X. Y. Huang, C. Y. Zhi, P. K. Jiang, D. Golberg, Y. Bando and T. Tanaka, *Adv Funct Mater*, 2013, **23**, 1824-1831.
- 156 H. B. Cho, N. C. Tu, T. Fujihara, S. Endo, T. Suzuki, S. Tanaka, W. H. Jiang, H. Suematsu, K. Niihara and T. Nakayama, *Mater Lett*, 2011, **65**, 2426-2428.
- 157 T. Fujihara, H. B. Cho, T. Nakayama, T. Suzuki, W. H. Jiang, H. Suematsu, H. D. Kim and K. Niihara, *J Am Ceram Soc*, 2012, **95**, 369-373.
- 158 H. B. Cho, Y. Tokoi, S. Tanaka, H. Suematsu, T. Suzuki, W. H. Jiang, K. Niihara and T. Nakayama, *Compos Sci Technol*, 2011, **71**, 1046-1052.
- 159 H. B. Cho, M. Mitsuhashi, T. Nakayama, S. Tanaka, T. Suzuki, H. Suematsu, W. H. Jiang, Y. Tokoi, S. W. Lee, Y. H. Park and K. Niihara, *Mater Chem Phys*, 2013, **139**, 355-359.
- 160 H. S. Lim, J. W. Oh, S. Y. Kim, M. J. Yoo, S. D. Park and W. S. Lee, *Chem Mater*, 2013, **25**, 3315-3319.

- 161 H. B. Cho, Y. Tokoi, S. Tanaka, T. Suzuki, W. H. Jiang, H. Suematsu, K. Niihara and T. Nakayama, *J Mater Sci*, 2011, **46**, 2318-2323.
- 162 T. Terao, C. Y. Zhi, Y. Bando, M. Mitome, C. C. Tang and D. Golberg, *J Phys Chem C*, 2010, **114**, 4340-4344.
- 163 C. Y. Zhi, Y. Bando, T. Terao, C. C. Tang and D. Golberg, *Pure Appl Chem*, 2010, **82**, 2175-2183.
- 164 J. Ravichandran, A. G. Manoj, J. Liu, I. Manna and D. L. Carroll, *Nanotechnology*, 2008, **19**, 085712.
- 165 S. K. Kisku and S. K. Swain, *J Am Ceram Soc*, 2012, **95**, 2753-2757.

Table I Comparison between properties of CNTs, graphene, BNNTs and BNNSs.

Materials	CNTs	Graphene	BNNTs	BNNSs
Color	Black	Black	White	White
Bonding	Covalent bonds; bonding length: 1.400-1.463 Å	Covalent bonds; bonding length: 1.4 Å	Covalent bonds with ionic component; bonding length: 1.437-1.454 Å	Covalent bonds with ionic component
Electronic structure	Metallic or semiconducting, dependent on chiralities	zero-gap semimetal with a tiny overlap between valence and conduction bands	5.0-6.0 eV band gap, independent of chiralities	5.0-6.0 eV band gap, independent of chiralities
Raman active modes	G band: 1580 cm ⁻¹ ; D band: 1350 cm ⁻¹ ; RBM model: (10, 10) CNT, 171.0 cm ⁻¹	G band: 1583 cm ⁻¹ ; 2D band: 2680 cm ⁻¹ ; the 2D band in single-layer graphene is much more intense and sharper than the one in multi-layer graphene	A1 tangential mode: 1370 cm ⁻¹ ; RBM model: (10, 10) BNNT, 153.0 cm ⁻¹	similar to h-BN, characteristic peak: 1365 cm ⁻¹
Mechanical properties	Young's Modulus :1.09-1.25 TPa; 0.84-0.99 TPa(theoretical) 0.27-0.95 TPa(experimental)	Young's Modulus: 1.0 Tpa (single-layer, experimental)	Young's modulus: 0.784-0.912 TPa; 0.71-0.83 TPa(theoretical) 0.5-0.7 TPa; 1.22 ± 0.24 TPa(experimental)	2D elastic modulus: 220-510 N/m (BNNSs with thicknesses of 1-2 nm)
Thermal conductivity (W/mK) at room temperature	~6000 (theoretical, SWCNT); >3000 (experimental, MWCNT, D~14 nm); ~1000 (experimental, MWCNT, D~10 nm); ~300 (experimental, MWCNT, D~35 nm)	3000-5000 (single-layer suspended graphene) ~600 (graphene supported on amorphous silica)	~180-300 (theoretical, SWBNNT); ~180-300 (experimental, MWBNNT);	300-2000 (theoretical) ~40 (experimental)
Thermal stability	Depends on sample, roughly between 500-700 °C	Depends on synthetic methods, 500-600 °C	High, up to 800-900 °C in air	superior to graphene

A comprehensive review of polymer composites of BN nanotubes and nanosheets with distinguished properties.

